Acute ethanol exposure reduces serotonin receptor 1A internalization by increasing ubiquitination and degradation of β-arrestin2

Received for publication, November 10, 2018, and in revised form, July 23, 2019 Published, Papers in Press, July 31, 2019, DOI 10.1074/jbc.RA118.006583

Deborah J. Luessen[‡], Haiguo Sun[‡], Molly M. McGinnis[‡], Michael Hagstrom[‡], Glen Marrs[§], Brian A. McCool[‡], and Rong Chen[‡§¶1]

From the [‡]Department of Physiology and Pharmacology and [¶]Center for the Neurobiology of Addiction Treatment, Wake Forest School of Medicine, Winston Salem, North Carolina 27157, and the [§]Center for Molecular Signaling, Department of Biology, Wake Forest University, Winston Salem, North Carolina 27106

Edited by Phyllis I. Hanson

Acute alcohol exposure alters the trafficking and function of many G-protein–coupled receptors (GPCRs) that are associated with aberrant behavioral responses to alcohol. However, the molecular mechanisms underlying alcohol-induced changes in GPCR function remain unclear. β-Arrestin is a key player involved in the regulation of GPCR internalization and thus controls the magnitude and duration of GPCR signaling. Although β-arrestin levels are influenced by various drugs of abuse, the effect of alcohol exposure on β-arrestin expression and β-arrestin–mediated GPCR trafficking is poorly understood. Here, we found that acute ethanol exposure increases β-arrestin2 degradation via its increased ubiquitination in neuroblastoma-2a (N2A) cells and rat prefrontal cortex (PFC). β-Arrestin2 ubiquitination was likely mediated by the E3 ligase MDM2 homolog (MDM2), indicated by an increased coupling between β-arrestin2 and MDM2 in response to acute ethanol exposure in both N2A cells and rat PFC homogenates. Importantly, ethanol-induced β-arrestin2 reduction was reversed by siRNA-mediated MDM2 knockdown or proteasome inhibition in N2A cells, suggesting β-arrestin2 degradation is mediated by MDM2 through the proteasomal pathway. Using serotonin 5-HT1A receptors (5-HT1ARs) as a model receptor system, we found that ethanol dose-dependently inhibits 5-HT1AR internalization and that MDM2 knockdown reverses this effect. Moreover, ethanol both reduced β-arrestin2 levels and delayed agonist-induced β-arrestin2 recruitment to the membrane. We conclude that β-arrestin2 dysregulation by ethanol impairs 5-HT1AR trafficking. Our findings reveal a critical molecular mechanism underlying ethanol-induced alterations in GPCR internalization and implicate β-arrestin as a potential player mediating behavioral responses to acute alcohol exposure.

Acute alcohol exposure produces a wide range of behavioral and neurobiological effects, including feelings of euphoria, loss of coordination, and cognitive impairment, which are thought to be key predictors of vulnerability to alcohol abuse in humans (1–3). This notion is further supported by a recent longitudinal study showing that individuals who exhibit higher sensitivity to the rewarding effect and lower sensitivity to the sedative effect of an initial acute alcohol exposure were more likely to develop symptoms of alcohol use disorders and escalate their alcohol consumption over time (4). Many aspects of behavioral responses to alcohol are mediated by various G-protein–coupled receptors (GPCRs).[2] For example, ethanol-induced locomotor stimulation is mediated by serotonin 5-HT_{1A} receptors (5-HT_{1A}Rs) because treatment with 5-HT_{1A}R agonist (8-OH-DPAT) reduced locomotor activity in response to an acute ethanol exposure (2.5 g/kg, i.p.) (5). Moreover, the sedative effect of ethanol is regulated by metabotropic glutamate receptor 5 (mGluR5) as genetic deletion of mGluR5 or treatment with the mGluR5 antagonist, 2-methyl-6-(phenylethynyl)pyridine, increases the duration of loss of righting reflex in mice acutely exposed to ethanol (6). Thus, elucidating the molecular mechanisms underlying ethanol-induced neuroadaptations in GPCRs is important for identifying potential new targets that mediate aberrant behavioral responses to alcohol.

β-Arrestin is an important modulator of GPCR internalization. Upon GPCR activation, β-arrestin is recruited to the receptor followed by uncoupling of the receptor from Gα-proteins and then a direct interaction with clathrin to induce receptor internalization. The rate and amplitude of GPCR internalization mediated by β-arrestin determine the duration and strength of GPCR signaling. Thus, a change in β-arrestin expression would alter receptor internalization, signaling, and receptor-mediated behavioral responses to ethanol. For instance, knockout of β-arrestin2 increases [^{35}S]GTPγS binding to cannabinoid type 1 receptors (CB1Rs) in the cortex, which is

This work was supported by National Institutes of Health Grants R01DA042862, P50DA006634, R01AA014445, F31AA025532, R01AA023999, T32AA007565, and F31AA025514. The authors declare that they have no conflicts of interest with the contents of this article. The content is solely the responsibility of the authors and does not necessarily represent the official views of the National Institutes of Health.

This article contains Figs. S1–S4.

[1] To whom correspondence should be addressed. Tel.: 336-716-8605; Fax: 336-716-8501; E-mail: rchen@wakehealth.edu.

[2] The abbreviations used are: GPCR, G-protein–coupled receptor; 5-HT_{1A}R, serotonin 5-HT1A receptor; CB1R, cannabinoid type 1 receptor; GRK, G-protein–coupled receptor kinase; N2A, neuroblastoma 2a; NEDD4, neural precursor cell expressed developmentally down-regulated protein 4; PFC, prefrontal cortex; ANOVA, analysis of variance; mGluR5, metabotropic glutamate receptor 5; GTPγS, guanosine 5′-3-*O*-(thio)triphosphate; HRP, horseradish peroxidase; 8-OH-DPAT, 8-hydroxy-2-(di-n-propylamino)tetralin.

presumably due to increased CB1R protein levels on the plasma membrane (7). The level of CB1R is known to be positively associated with ethanol consumption and preference (8, 9). The effect of acute or chronic ethanol exposure on β-arrestin expression is largely unknown with one exception. Chronic ethanol exposure was reported to increase β-arrestin mRNA and protein levels in the hippocampus and the striatum of alcohol-preferring rats after voluntary ethanol consumption (6% v/v, 21 days) compared with nonpreferring rats (10). The route, duration, and dose of ethanol exposure likely influence the effect of ethanol on β-arrestin expression. Thus, the first aim of this study was to examine the effect of acute ethanol exposure on β-arrestin expression using both cultured cells and rodent brains.

When GPCRs are internalized upon stimulation, β-arrestin dissociates from the internalized receptors. The dissociated β-arrestin either recycles to the membrane to promote additional cycles of internalization or enters proteasomes or lysosomes for degradation (11, 12). The endocytic fate of β-arrestin, recycling or degradation, is strongly controlled by post-translational modifications such as ubiquitination (13). Ubiquitination involves the sequential action of three enzymes: ubiquitin-activating E1 enzyme, ubiquitin-carrying E2 enzyme, and ubiquitin protein E3 ligase (14). When E3 ligases bind to their substrates, E2 enzymes are recruited to transfer ubiquitin molecules to the substrate (15). In various model systems, β-arrestin is capable of coupling to several E3 ligases, including MDM2 and neural precursor cell expressed developmentally down-regulated protein 4 (NEDD4) (16–18). For example, β-arrestin forms a complex with MDM2 in CHW cells, COS-7 cells, and mouse brain lysate, and this β-arrestin2–MDM2 interaction results in an increase in both basal and receptor-stimulated β-arrestin ubiquitination (16). However, ubiquitination is a reversible modification as linkages between ubiquitin and substrates are frequently hydrolyzed by deubiquitinating enzymes to maintain protein homeostasis and an available pool of free ubiquitin in the cell (19). E3 ligases can modify one or multiple lysine residues of a protein with either a single ubiquitin molecule (mono-ubiquitination) or ubiquitin polymers (poly-ubiquitination) (19). Emerging evidence suggests that poly-ubiquitination directs substrates to proteasomes for degradation, whereas mono-ubiquitination is primarily involved in protein trafficking (15, 20). It has been well-characterized that there is an increase in β-arrestin poly-ubiquitination when receptors are stimulated. For instance, activation of the β_2-adrenergic receptor in HEK293 and COS-7 cells increases β-arrestin poly-ubiquitination in an MDM2-dependent manner (11, 16). Additionally, treatment with antidepressants (*e.g.* citalopram) for 3 days or methamphetamine (10 μM) for up to 24 h enhances poly-ubiquitination of β-arrestin in C6 rat glioma and PC12 cells, respectively (21, 22). These data suggest that β-arrestin ubiquitination can be induced by various stimuli. Ubiquitinated β-arrestins are predominantly deubiquitinated and become available for subsequent recruitment to activated receptors; however, persistent ubiquitination of β-arrestin can lead to degradation (11, 21). Disruption of β-arrestin ubiquitination homeostasis could dysregulate the post-endocytic fate of β-arrestin and subsequent degradation, which will impact GPCR trafficking and activity. Thus, the second aim of this study was to determine the effect of acute ethanol exposure on β-arrestin ubiquitination and degradation as a potential mechanism for altered β-arrestin expression.

Acute ethanol exposure disrupts the trafficking of GPCRs in rodent brains and cultured neurons. For example, acute ethanol treatment (30 mM, 2 h) to rat hippocampus cultured neurons significantly increases $GABA_B$ receptor surface expression compared with the vehicle treatment (23). Moreover, acute ethanol administration (2.5 g/kg, p.o.) increases [^{3}H]DAMGO binding to μ-opioid receptors in rat PFC (24). However, the molecular mechanisms underlying ethanol-induced alterations in GPCR trafficking remain unclear. Because β-arrestin plays an important role in regulating the trafficking of many GPCRs, a change in β-arrestin expression and/or recruitment by ethanol exposure would influence receptor trafficking. We used 5-HT_{1A}Rs as a receptor model system to determine the effect of acute ethanol exposure on β-arrestin–mediated GPCR trafficking because the mechanism of 5-HT_{1A}R trafficking is well-characterized (25), and this receptor plays a role in mediating ethanol drinking behavior (26–28). This study showed for the first time that acute ethanol exposure increases proteasome-dependent β-arrestin2 degradation via MDM2 in both neuroblastoma 2a (N2A) cells and rat PFC. Furthermore, ethanol exposure abolished agonist-induced 5-HT_{1A}R trafficking that is likely attributed to dysregulation of β-arrestin2 expression and activity.

Results

Validation of β-arrestin2 antibody

We verified the specificity of a commercially available β-arrestin2 antibody in cells treated with β-arrestin2 siRNA. The protein levels of β-arrestin2 were assessed by Western blotting and immunocytochemistry. Knockdown of β-arrestin2 via siRNA significantly reduced β-arrestin2 protein levels by 63.43 ± 9.40% when compared with the control cells transfected with a corresponding scrambled siRNA (Fig. S1*A*, unpaired Student's *t* test, $p < 0.001$). Additionally, β-arrestin2 levels were also examined in knockdown and control cells by immunocytochemistry. There was a pronounced reduction of β-arrestin2 fluorescent intensity in β-arrestin2 siRNA-treated cells when compared with the scrambled siRNA treatment (Fig. S1*B*, unpaired Student's *t* test, $p < 0.01$).

Acute ethanol exposure reduces the total protein level of β-arrestin2 in N2A-5HT_{1A}R cells and rat PFC

We examined the effect of acute ethanol exposure on β-arrestin1/2 expression in both N2A cells and rat PFC. In N2A cells, β-arrestin1/2 levels were determined following the treatment with ethanol (15–75 mM) or vehicle (media) for 18 h without withdrawal (Fig. 1*A*). Data were normalized to the protein level of β-actin, which was not altered by ethanol treatment. A one-way ANOVA revealed a significant dose effect of ethanol on β-arrestin2 protein level, $F(3,20) = 5.796$, $p < 0.01$. Bonferroni post hoc analysis showed that 30 and 75 mM ethanol treatment significantly reduced β-arrestin2 levels by 44.8 ± 2.0 and 60.3 ± 1.7%, respectively, when compared with the vehicle treatment (Fig. 1*A*, $p < 0.01$). The β-arrestin1 protein levels

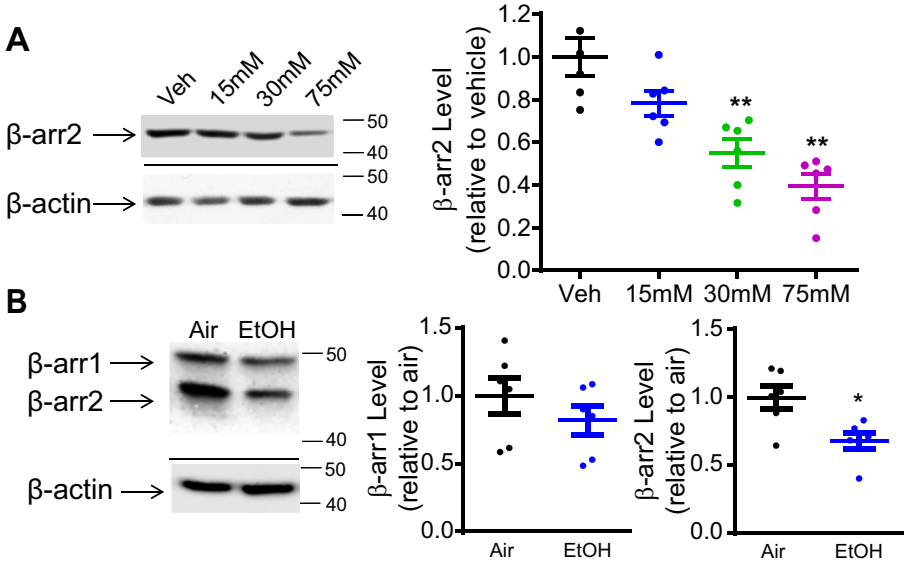

Figure 1. Acute ethanol treatment reduces the total level of β-arrestin2 protein in N2A-5HT1AR cells and rat PFC. *A,* representative Western blots and quantification of β-arrestin2 (*β-arr2*) protein levels in N2A-5HT1AR cells. Cells were acutely treated with ethanol (15–75 mM) or vehicle (*Veh*; media) for 18 h. The 30 and 75 mM ethanol treatment significantly reduced β-arrestin2 protein levels in N2A-5HT1AR cells ($n = 6$, **, $p < 0.01$ *versus* vehicle, a one-way ANOVA followed by Bonferroni post hoc test). *B,* representative Western blots and quantification of β-arrestin 1/2 protein levels in rat PFC. Rats were acutely exposed to ethanol vapor (*EtOH*) or control (*Air*) for 12 h followed by immediate sacrifice. Ethanol exposure significantly reduced β-arrestin2 protein level in rat PFC ($n = 6$, *, $p < 0.05$ *versus* air, unpaired Student's *t* test).

were not detectable in N2A cells with or without ethanol treatment. The reduced β-arrestin2 level was not due to toxicity induced by ethanol because the selected ethanol doses did not alter cell viability and membrane permeability measured by trypan blue assay (Fig. S2*A*) and immunocytochemistry, respectively (Fig. S2, *B* and *C*).

A similar effect was observed in the PFC of rats acutely exposed to ethanol vapor for 12 h without withdrawal (Fig. 1*B*). Ethanol exposure significantly reduced β-arrestin2 protein levels in the PFC by 32.4 ± 2.0% compared with the air exposure (Fig. 1*B*, unpaired Student's *t* test, $p < 0.05$). However, β-arrestin1 protein levels did not significantly differ between ethanol- and air-treated groups.

Acute ethanol exposure increases ubiquitination of β-arrestin2 in N2A-5HT$_{1A}$R cells and rat PFC

We further examined whether ethanol-induced reduction in β-arrestin2 levels was due to an increase in ubiquitination and subsequent degradation. First, immunocytochemistry was performed to measure the co-localization between fluorescently labeled β-arrestin2 (*green*) and ubiquitin (*red*) in N2A cells following 18 h of ethanol (15–75 mM) or vehicle (media) treatment (Fig. 2*A*). Co-localization was calculated as the number of spatially overlapped pixels (Fig. 2*A*, *yellow*) between β-arrestin2 (*green*) and ubiquitin (*red*) followed by conversion into a co-localization coefficient using FIJI software (National Institutes of Health). A one-way ANOVA indicated a significant effect of ethanol treatment on the co-localization between β-arrestin2 and ubiquitin, $F(3,116) = 14.87$, $p < 0.01$. Bonferroni post hoc analysis revealed that 30 and 75 mM ethanol treatment significantly increased this co-localization by 87.6 ± 2.1% (30 mM) and 201.9 ± 7.5% (75 mM) when compared with the vehicle treatment (Fig. 2*B*, $p < 0.01$).

We also performed immunoprecipitation assays as a complementary approach to immunocytochemistry to examine whether there was an increased coupling between ubiquitin and β-arrestin2 following ethanol exposure (30 mM; 18 h). First, to verify the specificity of the β-arrestin2 antibody used for immunoprecipitation, we immunoprecipitated β-arrestin2 in the presence or absence of a custom-made β-arrestin2–blocking peptide in drug-naïve N2A cells and rat PFC tissue. The blocking peptide completely eliminated signals produced by antibodies used to immunoblot for ubiquitin and β-arrestin2 from immunoprecipitated β-arrestin2 samples (Fig. 2*C*), suggesting the specificity of this β-arrestin2 antibody for immunoprecipitation. Then, we used this antibody to immunoprecipitate β-arrestin2 followed by immunoblotting for ubiquitin, which resulted in distinct mono-ubiquitination and poly-ubiquitination signals (Fig. 2*D*). We selected the ~60-kDa band as mono-ubiquitinated β-arrestin2 based on the presumed ~8-kDa upward shift in the molecular mass of β-arrestin2 caused by the addition of one ubiquitin chain. The poly-ubiquitination signal for β-arrestin2 present at a molecular mass of >80 kDa was consistent with reports from the literature (22, 29, 30). In N2A cells, we found that ethanol treatment increased both mono-ubiquitination and poly-ubiquitination of β-arrestin2 by 83.2 ± 1.7 and 83.6 ± 2.7%, respectively, compared with the vehicle treatment (Fig. 2, *E* and *F*, unpaired Student's *t* test, $p < 0.01$).

Similar to our observation in N2A cells, immunoprecipitation of β-arrestin2 in rat PFC homogenates showed that ethanol exposure significantly increased mono-ubiquitination by 46.8 ± 1.5% and poly-ubiquitination of β-arrestin2 by 50.9 ± 2.2% compared with the air treatment (Fig. 2, *I–K*), unpaired Student's *t* test, $p < 0.05$. Because the interaction between the protein substrate and E3 ligases facilitates protein ubiquitina-

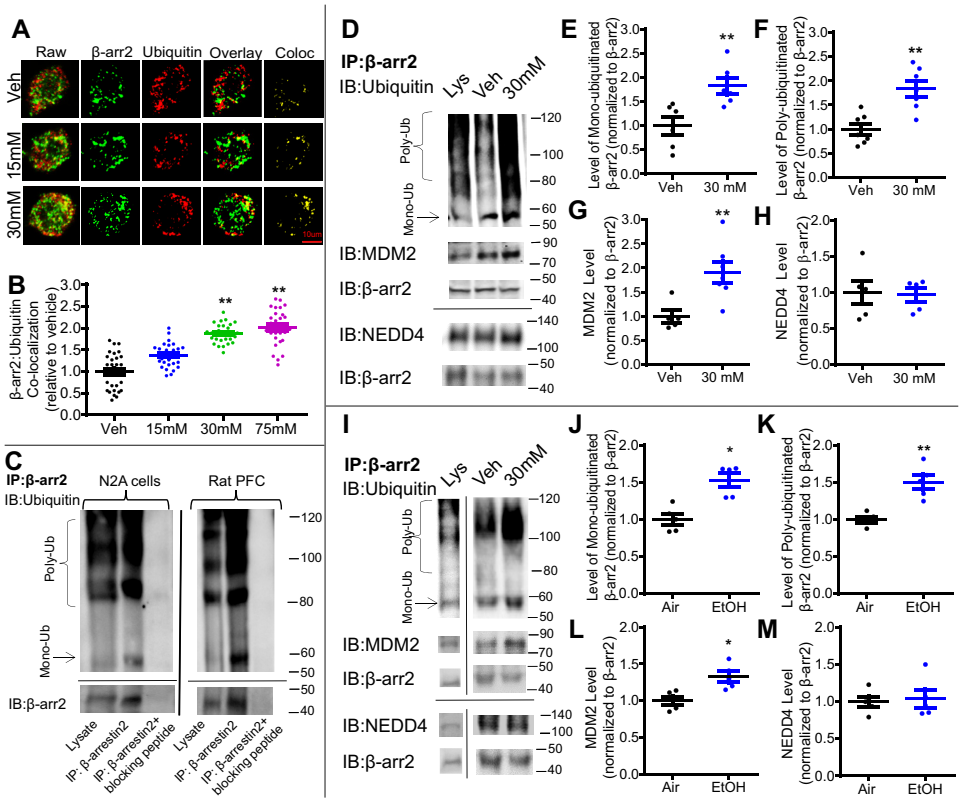

Figure 2. Acute ethanol exposure increases ubiquitination of β-arrestin2 in N2A-5HT1AR cells and rat PFC. *A,* representative raw and binary fluorescent images of β-arrestin2 (*green*) and ubiquitin (*red*) and co-localization (*Co-loc*) in N2A-5HT1AR cells treated with ethanol (15–75 mM) or vehicle (*Veh*) (media) for 18 h. *B,* ethanol exposure dose-dependently increased β-arrestin2 co-localization with ubiquitin ($n = 29–30$ cells/group, six replicates, **, $p < 0.01$ *versus* vehicle, a one-way ANOVA followed by Bonferroni post hoc test). *C,* validation of the rabbit anti-β-arrestin2 antibody (LSBio; LS-B15546) was performed using a custom-made blocking peptide (GenScript; sequence DDIVFEDFARLRLK). Immunoprecipitation (*IP*) was performed using lysates from drug-naïve N2A-5HT1AR cells and rat PFC tissue in the presence and absence of the corresponding β-arrestin2 (*β-arr*)-blocking peptide (10 μg). Immunoprecipitates and N2A cell lysates were immunoblotted (*IB*) for mouse anti-ubiquitin (Santa Cruz Biotechnology; sc8017) and mouse anti-β-arrestin2 (LSBio; LS-B6008). β-Arrestin2–blocking peptide abolished immunoreactive bands detected in samples without the presence of this blocking peptide. *D,* representative blots for immunoprecipitated β-arrestin2, ubiquitin, and MDM2 from N2A-5HT1AR cell lysates. Cells were treated with ethanol (30 mM, 18 h) or vehicle (*Veh*) (media), and cell lysates were immunoprecipitated overnight with rabbit anti-β-arrestin2 antibody. Immunoprecipitates and cell lysates were immunoblotted with mouse anti-ubiquitin, mouse anti-MDM2, rabbit anti-NEDD4, and mouse anti-β-arrestin2 antibodies. *E–H,* quantification of β-arrestin2 mono- and poly-ubiquitination, MDM2, and NEDD4 ($n = 5$, **, $p < 0.01$ *versus* vehicle, unpaired Student's *t* test). *I,* representative blots for immunoprecipitated β-arrestin2, ubiquitin, and MDM2 in rat PFC lysates. Samples from ethanol (*EtOH*) and control (*Air*) exposed rats were immunoprecipitated with rabbit anti-β-arrestin2 overnight. Immunoprecipitates and tissue lysates were immunoblotted with the antibodies described above. *J–M,* quantification of immunoprecipitated β-arrestin2, ubiquitin, MDM2, and NEDD4 ($n = 5$, *, $p < 0.05$ *versus* vehicle, unpaired Student's *t* test).

tion, we further assessed the strength of β-arrestin2 coupling to MDM2 in response to ethanol exposure. Ethanol exposure increased the association of MDM2 with immunoprecipitated β-arrestin2 by 91.1 ± 2.2 and 32.6 ± 1.3% in N2A cells and rat PFC, respectively, when compared with their corresponding control treatments (Fig. 2, *G* and *L*, unpaired Student's *t* test, $p < 0.05$). In contrast, ethanol exposure had no effect on the association of immunoprecipitated β-arrestin2 with another E3 ligase, NEDD4, in either model system (Fig. 2, *H* and *M*). It is also worth noting that the relative intensities of bands between mono- and poly-ubiquitinated β-arrestin2 in N2A cells were notably different from those in rat PFC tissues. This is likely attributed to differential expressions of various E2 and E3 ligases involved in ubiquitination of β-arrestin2 in each model. Additionally, bands located between mono- (~60 kDa) and poly-ubiquitinated β-arrestin2 (>80 kDa) likely reflect a spectrum of different ubiquitination states (bi-, tri-, tetra-ubiquitination, etc.) on individual lysine residues, as described previously (31). Because the role of these intermediate ubiquitination states is currently unclear, this study focused on mono- and poly-ubiquitination of β-arrestin2.

Acute ethanol exposure reduces β-arrestin2 protein expression via MDM2-mediated proteasomal degradation

Because there was an increased association of β-arrestin2 with MDM2 following ethanol exposure, we further determined whether MDM2 was involved in ethanol-induced degradation of β-arrestin2. To this end, MDM2 was knocked down via siRNA in N2A-5HT$_{1A}$R cells, and β-arrestin2 protein levels were measured after ethanol treatment (30–75 mM, 18 h) (Fig. 3*B*). MDM2 siRNA treatment reduced the MDM2 protein level by 57.8 ± 1.4% (Fig. 3*A*, unpaired Student's *t* test, $p < 0.05$) when compared with scrambled siRNA treatment. Furthermore, a two-way ANOVA revealed significant main effects of knockdown, $F(1,24) = 18.24$, $p < 0.01$; ethanol exposure, $F(2,24) = 7.70$, $p < 0.01$; and interaction, $F(2,24) = 4.67$, $p < 0.05$. Bonferroni post hoc analysis showed that MDM2 knockdown completely blocked ethanol-induced β-arrestin2 degra-

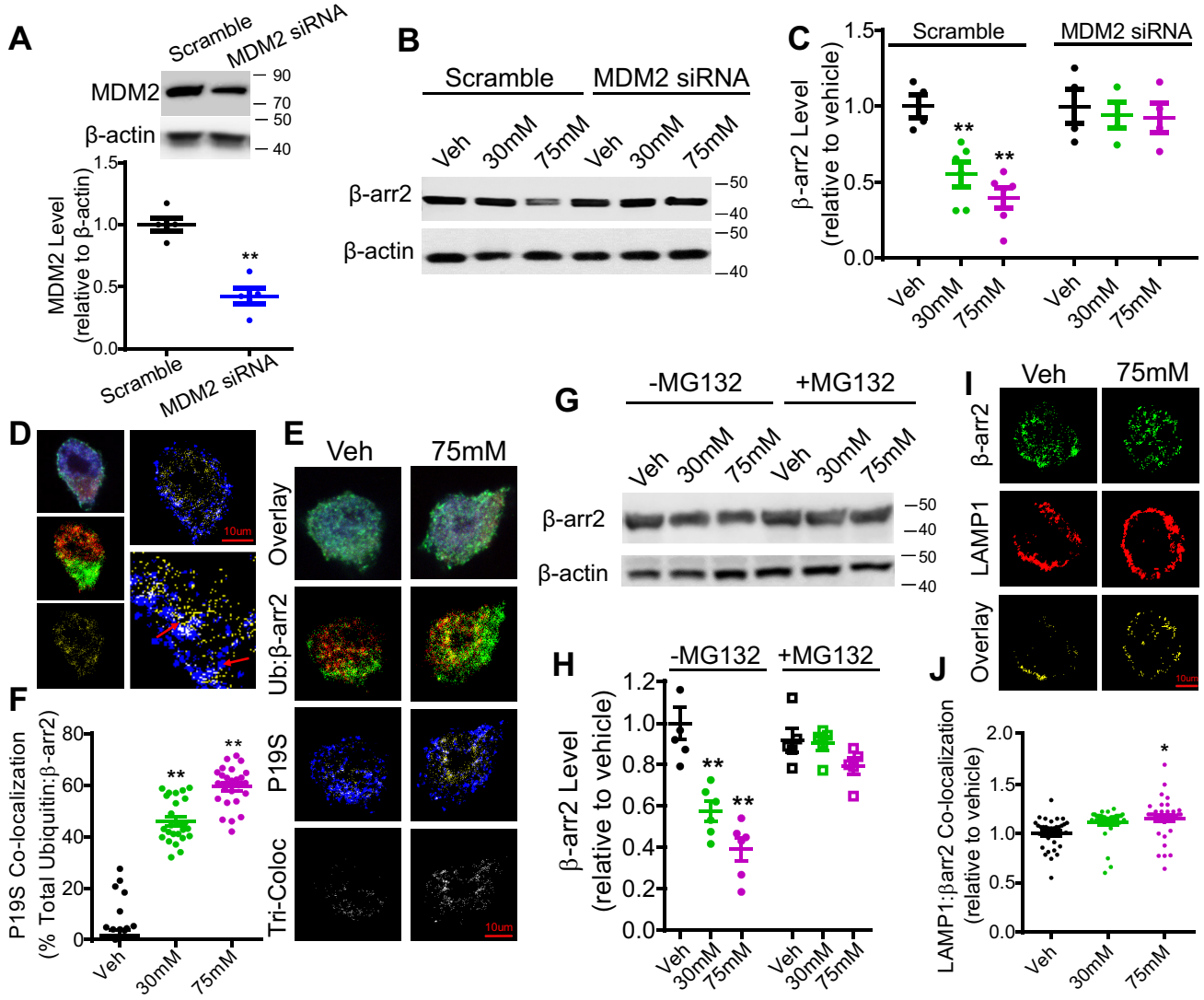

Figure 3. Acute ethanol exposure reduces β-arrestin2 protein expression in an MDM2- and proteasome-dependent manner in N2A-5HT1AR cells. *A,* verification of MDM2 protein knockdown via siRNA. N2A-5HT1AR cells were transfected with MDM2 siRNA or a corresponding scramble siRNA. MDM2 protein levels were measured 48 h after transfection by Western blotting. MDM2 siRNA treatment significantly reduced the endogenous MDM2 protein level when compared with scrambled siRNA-treated control cells ($n = 5$, **, $p < 0.01$ *versus* scramble, unpaired Student's *t* test). *B,* representative Western blotting of β-arrestin2 (*β-arr2*) protein level in scramble and MDM2 siRNA-treated cells. N2A-5HT1AR cells were transfected with MDM2 siRNA or a corresponding scramble siRNA and then treated with ethanol (30–75 mM) or vehicle (*Veh*) (media) for 18 h. Cell lysates were immunoblotted with rabbit anti-β-arrestin2 and goat anti-β-actin antibodies. *C,* quantification of β-arrestin2 levels in scramble and MDM2 siRNA-treated cells. MDM2 knockdown prevented ethanol-induced degradation of β-arrestin2 ($n = 6$, **, $p < 0.01$ *versus* vehicle, a two-way ANOVA followed by Bonferroni post hoc test). *D,* schematic illustration of spatial overlap analysis for quantitation of ubiquitin, β-arrestin2, and P19S co-localization. Co-localization between β-arrestin2 (*green*) and ubiquitin (*red*) was first determined as *yellow* overlapped pixels (*left, middle*). These co-localized pixels (*yellow; left, bottom*) were then isolated, and triple co-localization with P19S (*blue; right, top*) was determined as *white* overlapped pixels (*right, bottom*). Data were reported as a percentage of co-localization by overlapping pixel counts, $y/x + y + z$ (ubiquitin/β-arrestin2 co-localization with respect to P19S). *E,* representative confocal images of ubiquitin (*red*), β-arrestin2 (*green*), and P19S (*blue*) in N2A-5HT1AR cells after acute treatment with ethanol (15–75 mM,18 h) or vehicle (media). *Scale bars,* 10 μm. *F,* quantification of ubiquitin, β-arrestin2, and P19S co-localization. The co-localization of the ubiquitin, β-arrestin2, and P19S significantly increased after ethanol treatment (30–75 mM) ($n = 25$–28 cells/group, five replicates, **, $p < 0.01$ *versus* vehicle, a one-way ANOVA followed by Bonferroni post hoc test). *G,* representative Western blotting of β-arrestin2 levels in N2A-5HT1AR incubated with or without MG132 (5 μM) during treatment with ethanol (30–75 mM, 18 h) or vehicle (media). *H,* quantification of β-arrestin2 protein levels. Treatment with MG132 prevented acute ethanol-induced (30 and 75 mM) reduction in β-arrestin2 protein levels in N2A-5HT1AR cells ($n = 5$, **, $p < 0.01$ *versus* vehicle, a two-way ANOVA followed by Bonferroni post hoc test). *I,* representative confocal images of LAMP1 (*red*) and β-arrestin2 (*green*) in N2A-5HT1AR cells after acute treatment with ethanol (30–75 mM, 18 h) or vehicle (media). *Scale bars,* 10 μm. *J,* quantification of β-arrestin2 and LAMP1 co-localization. β-Arrestin2 co-localization with LAMP1 significantly increased after a high-dose ethanol treatment (75 mM) compared with vehicle treatment ($n = 35$ cells/group, five replicates, *, $p < 0.05$ *versus* vehicle, a one-way ANOVA followed by Bonferroni post hoc test).

dation when compared with scrambled siRNA treatment (Fig. 3, *B* and *C*, $p < 0.05$).

Previous studies showed that ubiquitination primarily directs β-arrestin2 for proteasome-dependent degradation in C6 glioma and PC12 cells (21, 22). Therefore, we performed immunocytochemistry to examine the co-localization between fluorescently labeled β-arrestin2, ubiquitin, and proteasome marker P19S in N2A-5HT$_{1A}$R cells (Fig. 3, *D–F*) following treatment with ethanol (30–75 mM, 18 h) or vehicle (media). Briefly, co-localization between β-arrestin2 (Fig. 3, *D–F*, *green*) and ubiquitin (*red*) was first determined as *yellow* overlapped pixels. Then the co-localization of β-arrestin2, ubiquitin, and

P19S was quantified as the spatial overlap between co-localized pixels (*yellow*) and P19S (*blue*), which was represented by *white* overlapped pixels (Fig. 3*D*). A one-way ANOVA indicated a significant effect of ethanol exposure on ubiquitin, β-arrestin2, and P19S co-localization, $F(2,12) = 54.48$, $p < 0.01$. Bonferroni post hoc analysis showed that 30 and 75 mM ethanol treatment significantly increased the co-localization of β-arrestin2, ubiquitin, and P19S by 44.5 ± 2.8% (30 mM) and 58.3 ± 2.5% (75 mM), respectively, when compared with the vehicle treatment (Fig. 3*F*, $p < 0.01$). To test whether the proteasome-dependent degradation pathway is the primary mechanism for ethanol-induced β-arrestin2 reduction, N2A-5HT$_{1A}$R cells were treated with the proteasome inhibitor MG132 (5 μM) or vehicle (media) in the presence or absence of ethanol (30–75 mM; 18 h) followed by measurement of β-arrestin2 levels (Fig. 3*G*). A two-way ANOVA revealed significant main effects of ethanol exposure, $F(2,24) = 19.64$, $p < 0.01$; proteasome inhibition, $F(1,24) = 19.19$, $p < 0.01$; and interaction, $F(2,24) = 9.70$, $p < 0.01$. Bonferroni post hoc analysis showed that MG132 treatment blocked β-arrestin2 degradation induced by ethanol exposure (30–75 mM) when compared with the vehicle treatment (Fig. 3*H*, $p < 0.01$).

To assess whether acute ethanol exposure also directed β-arrestin2 into lysosomes for degradation, we measured the co-localization between fluorescently labeled β-arrestin2 and a lysosome marker, LAMP1, following treatment with ethanol (30–75 mM, 18 h) or vehicle (media) (Fig. 3*I*). A one-way ANOVA showed a significant effect of ethanol exposure on the co-localization between β-arrestin2 and LAMP1, $F(2,102) = 4.87$, $p < 0.01$. Bonferroni post hoc analysis showed that only the high-dose ethanol treatment (75 mM) produced a small but significant increase in the co-localization of β-arrestin2 with LAMP1 by 14.0 ± 2.6% (Fig. 3*J*, $p < 0.05$). Collectively, these data suggest that acute ethanol exposure primarily directs β-arrestin2 to undergo the proteasome-dependent degradation; however, a small pool of β-arrestin2 can also be routed to lysosomes under specific conditions such as high doses of ethanol exposure.

Acute ethanol exposure inhibits agonist-induced 5-HT$_{1A}$R internalization

Because β-arrestin regulates internalization of many GPCRs, including 5-HT$_{1A}$R (32, 33), the functional consequence of ethanol-induced β-arrestin2 reduction on GPCR internalization was examined using 5-HT$_{1A}$R as a receptor model system. The internalization of 5-HT$_{1A}$R was measured by immunocytochemistry using an antibody-feeding protocol described previously (34). We first assessed the kinetics of 8-OH-DPAT–stimulated 5-HT$_{1A}$R internalization. It has been shown previously that 5-HT$_{1A}$R internalization occurs in a clathrin- and β-arrestin-dependent manner in LLC-PK1 cells (35). In N2A-5HT$_{1A}$R cells, pretreatment with dynasore or concanavalin A, inhibitors of dynamin- and clathrin-mediated internalization, respectively, completely inhibited internalization of the receptor (Fig. S3), indicating that 5-HT$_{1A}$R internalization is clathrin- and dynamin-dependent. Next, the effect of ethanol treatment (15–75 mM; 18 h) on 8-OH-DPAT–stimulated 5-HT$_{1A}$R internalization was determined (Fig. 4*A*). A two-way ANOVA revealed significant main effects of ethanol treatment, $F(3,577) = 79.36$, $p < 0.01$; time, $F(4,577) = 311.7$, $p < 0.01$; and interaction, $F(12,577) = 14.61$, $p < 0.01$. Although 8-OH-DPAT treatment (1 μM) caused a time-dependent 5-HT$_{1A}$R internalization in both vehicle- and ethanol-treated cells, Bonferroni post hoc analysis showed that treatment with 30 or 75 mM ethanol significantly inhibited 8-OH-DPAT–stimulated 5-HT$_{1A}$R internalization at the indicated time points when compared with the vehicle treatment (Fig. 4*B*, $p < 0.01$). Because there was an increase in MDM2 association with β-arrestin2 in response to acute ethanol exposure (Fig. 2), we examined whether dysregulated 5-HT$_{1A}$R internalization was mediated by increased β-arrestin2 ubiquitination and degradation by knocking down MDM2. A two-way ANOVA revealed significant main effects of knockdown, $F(1,214) = 11.62$, $p < 0.01$; ethanol treatment, $F(2,214) = 18.66$, $p < 0.01$; and interaction, $F(2,214) = 7.97$, $p < 0.01$. Bonferroni post hoc analysis showed that MDM2 siRNA knockdown abolished ethanol-induced attenuation of 5-HT$_{1A}$R internalization (Fig. 4*C*, $p < 0.01$), suggesting that MDM2-mediated degradation of β-arrestin2 directly impacts 5-HT$_{1A}$R internalization.

Ethanol exposure reduces and delays recruitment of β-arrestin2 to the plasma membrane

We also investigated whether ethanol-induced disruption of 5-HT$_{1A}$R internalization resulted from a deficit in β-arrestin2 recruitment to the membrane. The effect of acute ethanol exposure (15–30 mM; 18 h) on 8-OH-DPAT–stimulated β-arrestin2 translocation was examined by performing a segmentation analysis of the redistribution of fluorescently-labeled β-arrestin2 as described previously (Fig. 5*A*) (34). This method is commonly used to measure the translocation of fluorescently labeled proteins to the membrane (36, 37). Briefly, the outer boundary of each cell was defined by the localization of fluorescently labeled surface 5-HT$_{1A}$Rs, and the inner boundary was marked as a standardized 2-μm distance from the outer boundary. Accordingly, the outer segment was calculated as the cellular area between the outer and inner boundaries, and the remaining cellular area within the inner boundary was indexed as the inner segment. A one-way ANOVA showed a significant effect of ethanol treatment on the basal level of β-arrestin2 membrane localization, $F(2,84) = 8.85$, $p < 0.01$. Bonferroni post hoc analysis revealed that the baseline β-arrestin2 membrane localization was reduced after ethanol treatment (30 mM) compared with the vehicle treatment (Fig. 5*C*, $p < 0.01$). We also examined β-arrestin2 membrane recruitment upon 5-HT$_{1A}$R stimulation by 8-OH-DPAT (1 μM). A two-way ANOVA revealed significant main effects of treatment time, $F(3,336) = 37.19$, $p < 0.01$, and interaction, $F(6,336) = 9.67$, $p < 0.01$. Bonferroni post hoc analysis showed that 8-OH-DPAT stimulation in vehicle-treated cells significantly increased the redistribution of β-arrestin2 into the outer segment (55 ± 3.2%) as early as 5 min (Fig. 5*D*, $p < 0.01$). However, 8-OH-DPAT stimulation in ethanol-treated cells (30 mM, 18 h) did not show a significant increase in β-arrestin2 redistribution into the outer segment (31.7 ± 4.0%) until 15 min. Taken together, these findings indicate that acute ethanol exposure reduced and delayed 8-OH-DPAT–stimulated β-arrestin2 membrane

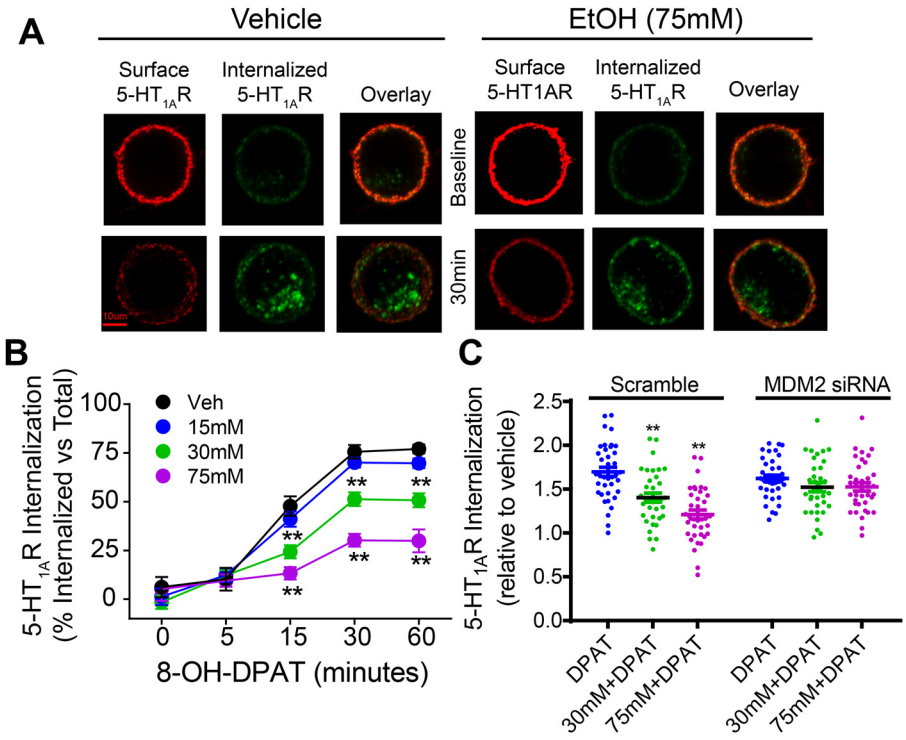

Figure 4. Acute ethanol exposure inhibits agonist-induced 5-HT1AR internalization. N2A-5HT1AR cells were acutely treated with ethanol (15–75 mM, 18 h) or vehicle (*Veh*) (media) followed by labeling the surface 5-HT1ARs with mouse anti-HA antibody. Then cells were warmed to 37 °C and treated with 8-OH-DPAT (1 μM) for the indicated time points to induce internalization. At the end of each time point, the remaining primary antibody-bound surface 5-HT1ARs that did not internalize were labeled with goat anti-mouse Alexa 647 (*red*). Internalized intracellular 5-HT1ARs were identified by labeling with goat anti-mouse Alexa 405 (*blue,* pseudo-colored to *green*). *A,* representative confocal images of surface and internalized 5-HT1ARs from vehicle- and ethanol-treated cells (15–75 mM). *Scale bar,* 10 μm. *B,* quantification of 8-OH-DPAT–stimulated 5-HT1AR internalization. Internalized 5-HT1ARs were calculated as percent of their own total surface 5-HT1AR intensity. Receptor internalization occurred in a time-dependent manner in both vehicle- and ethanol-treated cells ($n = 47–50$ cells/group, five replicates, **, $p < 0.01$ *versus* vehicle , a two-way ANOVA followed by Bonferroni post hoc test). Ethanol treatment (30–75 mM) significantly inhibited 8-OH-DPAT–stimulated 5-HT1AR internalization compared with the vehicle treatment. Data are normalized and expressed relative to vehicle. *C,* MDM2 siRNA knockdown blocked the inhibition of 5-HT1AR internalization after ethanol (30–75 mM, 18 h) or vehicle (media) treatment ($n = 35–38$ cells/group, six replicates, **, $p < 0.01$ *versus* scramble, a two-way ANOVA followed by Bonferroni post hoc test).

translocation, which likely explains the abolished agonist-induced internalization of 5-HT_{1A}R following acute ethanol exposure.

Discussion

In this study, we show for the first time that acute ethanol exposure reduced β-arrestin2 expression level via MDM2-mediated ubiquitination and degradation. An important functional consequence of ethanol-induced dysregulation of β-arrestin2 was the abolished 5-HT_{1A}R internalization stimulated by agonist, which was likely impacted by delayed and reduced β-arrestin2 recruitment to the membrane upon 5-HT_{1A}R stimulation.

Drugs of abuse such as morphine, heroin, and methamphetamine modulate the expression of β-arrestin (22, 38, 39); however, there is very little knowledge about the effect of ethanol exposure on β-arrestin expression. In this study, we observed a notable reduction in β-arrestin2 levels in N2A-5HT_{1A}R cells and rat PFC following acute ethanol exposure. β-Arrestin degradation is regulated by ubiquitination, which occurs rapidly in response to various stimuli (13, 21). Herein, acute ethanol exposure increases β-arrestin2 ubiquitination in both N2A-5HT_{1A}R cells and rat PFC as evidenced by a marked increase in both mono- and poly-ubiquitination of β-arrestin2. Previous reports have focused exclusively on poly-ubiquitination of β-arrestin2 in response to stimulation of various types of receptors and other stimuli (16, 29, 30). Poly-ubiquitination is considered an important signal that directs proteins, such as β-arrestin, into proteasomes for degradation and can be induced by a diverse array of stimuli (15, 40). For instance, chronic antidepressant treatment increases poly-ubiquitination of β-arrestin2, which facilitates P26S proteasome-dependent degradation of β-arrestin2 in C6 rat glioma cells (21). Furthermore, poly-ubiquitination and subsequent proteasome-dependent degradation of β-arrestin occur in response to acute methamphetamine treatment (1 μM, 5 min) in PC-12 cells (22). In line with these observations, we found that ethanol exposure dose-dependently increased sorting of β-arrestin2 into proteasomes, and inhibition of proteasome activity prevented ethanol-induced degradation of β-arrestin2, suggesting that ethanol degrades β-arrestin2 via the proteasome-dependent pathway. Interestingly, we also observed increased co-localization of β-arrestin2 with the lysosomal marker LAMP1 only with high-dose (75 mM) ethanol treatment in N2A-5HT_{1A}R cells, suggesting that a subpopulation of β-arrestin2 can also be subject to lysosome-dependent degradation under specific conditions.

β-Arrestin is capable of coupling to several E3 ligases, including MDM2, for induction of β-arrestin ubiquitination (16). We found that acute ethanol exposure increased the complex for-

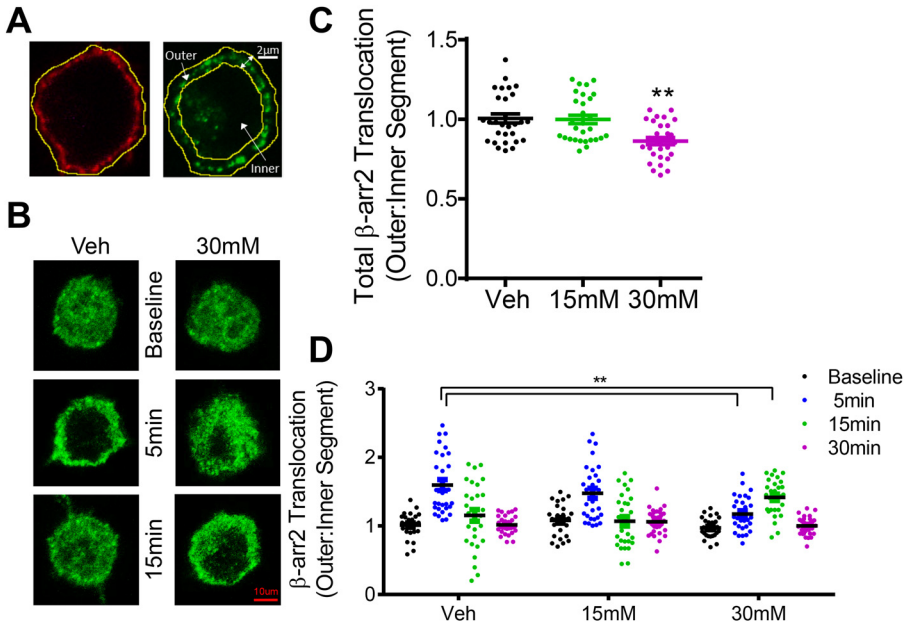

Figure 5. Acute ethanol exposure reduces and delays recruitment of β-arrestin2 to the plasma membrane. N2A-5HT1AR cells were treated with ethanol (15–30 mM, 18 h) or vehicle (*Veh*) (media) followed by stimulation with 8-OH-DPAT (1 μM for 5, 15, or 30 min). Surface 5-HT1ARs and cytosolic β-arrestin2 were fluorescently labeled as described under "Experimental procedures." *A,* schematic illustration of manual segmentation for quantitation of β-arrestin2 (*β-arr2*) translocation toward and away from the membrane. The outer boundary of each cell was manually outlined based on the localization of surface 5-HT1AR staining (*left, red*). An inner boundary was defined as a standardized 2-μm distance from the outer boundary. The outer sector was determined as the area between the outer and inner boundary, and the inner sector was determined as the remaining cellular area toward the cell center starting at the indicated inner boundary (*right*). β-Arrestin2 translocation from the membrane to the cytoplasm was calculated as the ratio of the outer to the inner sector intensity. *B,* representative confocal images of β-arrestin2 localization from ethanol (15–30 mM) and vehicle (*Veh*) (media)-treated cells. *Scale bars,* 10 μm. *C,* quantification of β-arrestin2 membrane localization. The level of β-arrestin2 membrane localization following 30 min of 8-OH-DPAT stimulation was reduced in cells treated with 30 mM ethanol compared with vehicle treatment ($n = 28–30$ cells/group, five replicates, **, $p < 0.01$ *versus* vehicle, a one-way ANOVA followed by Bonferroni post hoc test). *D,* ethanol treatment (30 mM) delayed β-arrestin2 membrane translocation. 8-OH-DPAT stimulation to control cells significantly increased the redistribution of β-arrestin2 into the outer segment as early as 5 min; however, 8-OH-DPAT stimulation to ethanol-treated cells (30 mM, 18 h) did not increase β-arrestin2 redistribution into the outer segment until 15 min ($n = 28–30$ cells/group, five replicates, **, $p < 0.01$ *versus* vehicle, a two-way ANOVA followed by Bonferroni post hoc test).

mation between β-arrestin2 and MDM2, but not NEDD4, in N2A-5HT$_{1A}$R cells and rat PFC, suggesting a unique involvement of MDM2 in regulation of enhanced β-arrestin2 ubiquitination and subsequent degradation induced by ethanol exposure. This notion is further substantiated by our observation that knockdown of MDM2 prevented ethanol-induced degradation of β-arrestin2 in N2A-5HT$_{1A}$R cells. It has been reported that phosphorylation of MDM2 or its substrates can enhance their interaction (41). Exposure to drugs of abuse, such as morphine, has been shown to increase β-arrestin2 phosphorylation (42). Therefore, future studies are necessary to determine whether ethanol exposure increases phosphorylation of β-arrestin2 and/or MDM2, which could be a potential mechanism for the increased association between these two proteins.

Given the important role of β-arrestin in regulating internalization of many GPCRs, the altered β-arrestin level by ethanol exposure would likely impact receptor internalization and function. In fact, we found that acute ethanol exposure blocked agonist-induced 5-HT$_{1A}$R internalization in a dose-dependent manner. It has been shown that 5-HT$_{1A}$R internalization requires β-arrestin as overexpression of a dominant-negative β-arrestin mutant, V53D, attenuates 5-HT$_{1A}$R internalization in HEK293 cells (32). Thus, the reduced β-arrestin level by ethanol exposure likely contributes to inhibition of 5-HT$_{1A}$R internalization. Although it has been reported that 5-HT$_{1A}$R internalization can increase or decrease following chronic ethanol exposure depending on ethanol dose, duration, and length of withdrawal (43, 44), this is the first observation of acute ethanol exposure, which leads to inhibition of agonist-stimulated 5-HT$_{1A}$R internalization. Because recruitment of β-arrestin to receptors is a critical step in receptor internalization, ethanol-induced disruption in β-arrestin recruitment could also account for decreased 5-HT$_{1A}$R internalization. We found that ethanol treatment reduced and delayed β-arrestin2 recruitment to the membrane upon 5-HT$_{1A}$R stimulation. Both factors contribute to the abolished 5-HT$_{1A}$R internalization induced by agonist stimulation. These data may underlie altered behavioral responses to ethanol mediated by receptors such as 5-HT$_{1A}$R and mGluR5.

The diminution of β-arrestin2 localization at the membrane is due to a reduction in the total β-arrestin2 levels induced by ethanol exposure. The delayed recruitment of β-arrestin2 may have resulted from enhanced mono-ubiquitination of β-arrestin2. Mono-ubiquitination disrupts protein trafficking through a number of distinct mechanisms, such as altering interactions between the substrate proteins and trafficking machinery or acting as a sorting signal to direct the movement of the substrate protein between different cellular compartments (45–48). For example, mono-ubiquitination delays the recruitment of Jen1, a monocarboxylate transporter, to multivesicular bodies (47). Mono-ubiquitination was also shown to increase trafficking of the Gα_s subunit into Rab5-positive endosomes (49).

Therefore, identification of the mono-ubiquitinated site and site-directed mutagenesis will help delineate the role of β-arrestin2 mono-ubiquitination in regulation of β-arrestin2 trafficking. Additionally, it was reported that the expression level of β-arrestin regulates the rate and extent of β-arrestin recruitment to activated GPCRs. For instance, β2AR-stimulated β-arrestin2 recruitment is significantly greater and displays a biphasic pattern of recruitment (fast recruitment followed by slow recruitment) in HEK293 cells with a high expression of β-arrestin2 compared with cells with low β-arrestin2 expression (50). Therefore, reduced β-arrestin2 expression level after ethanol exposure may contribute to both delayed and reduced β-arrestin2 membrane recruitment in response to 5-HT_{1A}R stimulation. Finally, there are other potential factors that may also be involved in β-arrestin2 membrane translocation, including changes in levels of GPCRs and other endocytic proteins, such as G-protein–coupled receptor kinases (GRKs) (33, 51). However, we did not observe alterations in the total protein levels of HA-5HT_{1A}R or GRK2 in N2A-5HT_{1A}Rs cells treated with ethanol (15–75 mM) when compared with the vehicle treatment (Fig. S4). Furthermore, receptor phosphorylation is an important regulator of β-arrestin membrane recruitment (52); therefore, future studies should focus on whether ethanol exposure alters phosphorylation of 5-HT_{1A}R.

In summary, this study provides for the first time evidence that acute ethanol exposure abolishes 5-HT_{1A}R internalization through enhanced MDM2-dependent β-arrestin2 ubiquitination and proteasome-dependent degradation. These findings may be applicable to other GPCRs whose internalization is β-arrestin–dependent. These β-arrestin–mediated changes in GPCR activity may be relevant to behavioral desensitization and/or tolerance to ethanol exposure.

Experimental procedures

Animals

Male Sprague-Dawley rats (Envigo) were housed in pairs and maintained on a 12:12 h light/dark cycle (lights on at 9 p.m.) with food and water *ad libitum*. Animals were ~10–11 weeks of age (300–350 g) upon arrival. After 7 days of habituation, animals were exposed to ethanol or air as described previously (53, 54). Briefly, animals were placed into air-tight Plexiglas chambers (Triad Plastics) in their home cages and were exposed to either ethanol vapor or room air during the light cycle for 12 h. Ethanol vapor, produced by submerging an air stone in 95% ethanol, was mixed with room air and was pumped into the chambers at a rate of 16 liters/min. Ethanol levels were maintained at ~35 mg/liter within the chamber. All animals were euthanized immediately following 12 h of ethanol or air exposure. Blood ethanol concentrations determined from the trunk blood were 242.3 ± 21.3 mg/dl at the time of sacrifice. Blood ethanol concentrations were determined using a standard, commercially available ethyl alcohol enzymatic assay kit (Carolina Liquid Chemistries; catalog no. BL421). All animal care procedures were in accordance with the National Institutes of Health Guide for the Care and Use of Laboratory Animals and approved by the Wake Forest Animal Care and Use Committee.

Generation of N2A-5-HT_{1A}R stable cell line

Parental N2A cells (ATCC) were grown in Opti-MEM media supplemented with 10% fetal bovine serum, 100 units/ml penicillin, and 100 μg/ml streptomycin. To generate a cell line stably expressing HA-5HT_{1A}R, N2A cells were transfected with human 5-HT_{1A}R cDNA with an HA-tag at the N terminus (HA-5-HT_{1A}R; Missouri S&T cDNA Resource Center) using Lipofectamine 2000 (Invitrogen) followed by an antibiotic selection with geneticin G418 (400 μg/ml). The expression of HA-5-HT_{1A}Rs was confirmed by the mRNA level and the protein presence using quantitative PCR and immunocytochemistry, respectively.

N2A-5HT_{1A}R cells were subject to fluorescence-activated cell sorting (FACS) to isolate cells with a high expression of HA-tagged 5HT_{1A}R. Briefly, cells suspended in ice-cold PBS containing 3% BSA, at ~5×10^6 viable cells/ml, were incubated with HA-tag DyLight488-conjugated antibody (Columbia Biosciences; D8–1830) on ice for 1 h. Then cells were washed three times by centrifugation at 400 × *g* for 5 min. Cells were resuspended in ice-cold PBS, 10% fetal bovine serum and sorted using a FACS Aria cell sorter (BD Biosciences). Live cells were gated based on forward/side scatter, and events in the top 3–4% of 488 nm fluorescence were selected, cultured, and expanded in medium containing geneticin (400 μg/ml).

Acute ethanol treatment to N2A-5-HT_{1A}R cells

N2A-5HT_{1A}R cells were treated with ethanol (15, 30, or 75 mM) or vehicle (media) for 18 h. Ethanol-treated cell culture plates were placed in a closed but not sealed polystyrene box with an open dish containing the corresponding concentration of ethanol. As shown previously, this procedure results in stable ethanol levels for several days (55, 56). The concentration of ethanol in the culture medium was determined using a colorimetric ethanol assay (Bioassay Systems; ECET100), which was performed at the end of the 18-h treatment period. Under these growing conditions, the average reduction in ethanol concentration after 18 h for each dose of ethanol was 3.13 ± 0.85% compared with initial ethanol concentrations at the time of treatment (not significant, $p = 0.24$ *versus* initial treatment, paired Student's *t* test, $n = 6$).

Validation of a β-arrestin2 antibody for Western blotting and immunocytochemistry

We verified the specificity of a commercially available β-arrestin2 antibody (LSBio; LS-B15546) in cells treated with β-arrestin2 siRNA. N2A-5HT_{1A}R cells were transiently transfected with 5 nM β-arrestin2 siRNA (Santa Cruz Biotechnology; sc-29743) or scrambled siRNA (Santa Cruz Biotechnology; sc-37007). Cells were lysed 48 h after transfection, and the protein concentrations were determined using BCA protein assay (Thermo Fisher Scientific). Protein (20 μg) was loaded on 10% Tris-glycine gels for SDS-PAGE and then was transferred to nitrocellulose membranes. β-Arrestin2 proteins were probed with β-arrestin2 antibody (LSBio; LS-B15546) followed by goat anti-rabbit IgG HRP (Santa Cruz Biotechnology; sc-2005). β-Actin (Santa Cruz Biotechnology; sc-1616) was used as an internal control. Bands were visualized using the chemiluminescence detection method (Pierce; catalog no. 32106). The

intensity of β-arrestin2 immunoreactive bands was normalized to β-actin and expressed as relative to the scrambled siRNA control.

Additionally, β-arrestin2 siRNA knockdown and scrambled siRNA-treated control cells were analyzed by immunocytochemistry. Cells were fixed with 4% formaldehyde for 15 min and permeabilized with the blocking buffer containing 6% normal horse serum and 0.01% Triton X-100 for 10 min. Then cells were incubated with the rabbit anti-β-arrestin2 antibody (LS-B15546) followed by goat anti-rabbit Alexa 488 antibody. Coverslips were mounted using Prolong Gold Antifade reagent with 4,6-diamidino-2-phenylindole (Invitrogen; P36931). Fluorescence was imaged by a Zeiss LSM 880 confocal microscope.

MDM2 protein knockdown via siRNA

N2A-5HT$_{1A}$R cells were transiently transfected with a mouse MDM2 siRNA (Mm01_00139357) or a corresponding scrambled siRNA obtained from Sigma. Cells were lysed in solubilization buffer containing 50 mM Tris-HCl (pH 7.4), 150 mM NaCl, and 1% Triton X-100. Western blotting was performed to determine MDM2 levels using mouse anti-MDM2 antibody (Millipore; OP46) followed by a horse anti-mouse HRP-conjugated secondary antibody (Cell Signaling Technology, catalog no. 7076). Bands were visualized using chemiluminescence detection method (Pierce; catalog no. 32106). Quantification of the bands was performed using ImageJ (National Institutes of Health). MDM2 immunoreactive bands were normalized to β-actin (Santa Cruz Biotechnology) and expressed as relative to the scrambled siRNA control.

Confocal microscopy

Fluorescent images were acquired with Zeiss LSM 710 and 880 laser-scanning confocal microscopes. Confocal image planes were acquired with a ×63/NA 1.4 PlanApo oil-immersion objective. Alexa 405, Alexa 555, and Alexa 647 signals were excited at 405, 561, and 633 nm with diode-pumped solid-state (DPSS), and HeNe lasers, respectively. Fluorescent channels were acquired sequentially to prevent cross-excitation of laser signal and to minimize bleed-through. All images were acquired with identical settings for excitation intensity, detector sensitivity, and pinhole to allow intensity comparison between samples. Images for analysis were obtained by taking a *z* axis stack of image planes (1024 × 1024 pixels) with 0.2-μm steps encompassing the entire cell structure. Fluorescent intensity was quantitated for each channel using ImageJ software (National Institutes of Health). All images were adjusted with Gaussian blur for presentation purposes only. Alexa 405 emission was pseudocolored as green upon acquisition for optimal presentation appearance. All experiments were performed independently at least four times. For each group, ~25–35 cells were selected for analysis from each experiment.

Immunocytochemistry

Stimulated 5-HT$_{1A}$R internalization following treatment with ethanol (15–75 mM) or vehicle (media) for 18 h in N2A-5HT$_{1A}$R cells was measured using an antibody feeding technique, as described previously (34). N2A-5HT$_{1A}$R cells were washed with PBS and blocked with 6% normal horse serum in PBS at 4 °C for 30 min. Surface 5-HT$_{1A}$Rs were then labeled with mouse anti-HA tag (Sigma; H6958) for 45 min at 4 °C. Cells were warmed to 37 °C and stimulated with 8-OH-DPAT (1 μM) for 5, 15, 30, or 60 min. Internalization was terminated by washing cells with cold PBS and placing coverslips on ice. The remaining primary antibody-bound surface 5-HT$_{1A}$Rs were incubated with rabbit anti-mouse Alexa 647 to determine the pool of surface 5-HT$_{1A}$Rs that were not internalized. Next, cells were fixed with 4% formaldehyde for 15 min and permeabilized with 0.1% Triton X-100 for 10 min. Internalized 5-HT$_{1A}$Rs bound with HA-tag primary antibody were labeled with goat anti-mouse Alexa 405 for quantification of internalized 5-HT$_{1A}$Rs. Stimulated 5-HT$_{1A}$R internalization was calculated as the percent fluorescent intensity of Alexa 405 (internalized 5-HT$_{1A}$Rs) of the total (Alexa 647 + Alexa 405) (total surface 5-HT$_{1A}$Rs before internalization). Data were presented as relative to the baseline level of 5-HT$_{1A}$R internalization in vehicle-treated cells.

We examined the co-localization of β-arrestin2, ubiquitin, and the proteasome marker P19S. Briefly, cells were pretreated with ethanol (15–75 mM) or vehicle (media) for 18 h, then washed with cold PBS prior to fixation with 4% formaldehyde for 15 min, and permeabilized with 0.1% Triton X-100 in blocking buffer containing 6% normal horse serum for 10 min. After blocking with 6% normal horse serum in PBS for 20 min, cells were incubated with the following antibodies: rabbit anti-β-arrestin2 (LSBio; LS-B15546), sheep anti-ubiquitin (LSBio; LS-C76671), and goat anti-P19S (Novus Biologicals; NB100-1483) for 1 h followed by incubation with the secondary antibodies donkey anti-goat Alexa 633, donkey anti-sheep Alexa 555, and goat anti-rabbit Alexa 405, respectively. All fluorescent secondary antibodies are from Invitrogen. Coverslips were mounted using Prolong Gold mounting reagent (Invitrogen, P36930) and imaged via confocal microscopy. Images were processed, and spatial overlap was calculated using FIJI and Photoshop. To directly assess spatial overlap of these proteins, background was removed, and variable intensity information from each image was done by thresholding. This method allows each pixel to provide binary information for the presence or absence of each protein and to provide specific quantitation and display of positional overlap. The co-localization between β-arrestin2 (green) and ubiquitin (red) was first determined as yellow overlapped pixels. These co-localized pixels (yellow) were then isolated, and triple co-localization with P19S (blue) was determined as white overlapped pixels. Data were reported as a percentage of co-localization by overlapping pixel counts, $y/x + y + z$, (ubiquitin/β-arrestin2 co-localization with respect to P19S).

Western blotting

β-Arrestin levels were measured in N2A-5HT$_{1A}$R cells and rat PFC tissue, and GRK2 and HA-tagged 5-HT$_{1A}$R levels were measured in N2A-5HT$_{1A}$R cells only. N2A-5HT$_{1A}$R cells were lysed in solubilization buffer (50 mM Tris-HCl (pH 7.4), 150 mM NaCl, and 1% Triton X-100), and rat PFC tissue was homogenized in RIPA buffer containing 25 mM Tris-HCl (pH 7.4), 150 mM NaCl, 0.1% SDS, 0.5% sodium deoxycholate, and 1% Triton X-100. Lysates were resolved by SDS-PAGE and transferred to

nitrocellulose membrane. Membranes were immunoblotted with rabbit anti-β-arrestin antibody (LSBio; LS-B15546), mouse anti-GRK2 (Santa Cruz Biotechnology; sc-13143), or mouse anti-HA tag (GenScript, A01244) followed by a goat anti-rabbit HRP-conjugated secondary antibody (Santa Cruz Biotechnology; sc-2005) or horse anti-mouse HRP-conjugated secondary antibody (Cell Signaling Technology, catalog no. 7076), respectively. β-Actin (Santa Cruz Biotechnology; sc-1616) was used as an internal control. Bands were visualized using chemiluminescence detection method (Pierce; catalog no. 32106). Quantification of the bands was performed using ImageJ (National Institutes of Health). The intensity of β-arrestin immunoreactive bands was normalized to that of β-actin and expressed as relative to the control.

To evaluate whether ethanol-induced β-arrestin2 degradation was proteasome-dependent, cells were incubated with or without MG132 (5 μM), a proteasome inhibitor as shown previously (57), during treatment with ethanol (30–75 mM) or vehicle for 18 h. Western blotting was performed to measure β-arrestin2 protein levels.

Immunoprecipitation

To examine β-arrestin2 ubiquitination, N2A-5HT$_{1A}$R cells and rat PFC tissue were solubilized in a lysis buffer containing 50 mM NaCl, 50 mM HEPES (pH 7.2), 10% glycerol, 1 mM EGTA, 1 mM EDTA, 10 mg/ml iodoacetamide, 1% Triton X-100, or RIPA buffer containing 25 mM Tris-HCl (pH 7.4), 150 mM NaCl, 0.1% SDS, 0.5% sodium deoxycholate, and 1% Triton X-100, respectively, supplemented with 10 mM *N*-ethylmaleimide for 1 h on ice. Samples were incubated with rabbit anti-β-arrestin2 antibody (LSBio; LS-B15546), conjugated with protein A/G beads (Santa Cruz Biotechnology) at 4 °C overnight. Samples were washed, and the immunoprecipitated proteins were eluted with the sample buffer containing dithiothreitol (DTT). The proteins were separated on a 10% SDS-polyacrylamide gel and transferred to nitrocellulose membranes for sequential Western blotting with mouse anti-MDM2 (Millipore; OP46), mouse anti-ubiquitin (Santa Cruz Biotechnology; sc8017), and then mouse anti-β-arrestin2 (LSBio; LS-B6008). In an additional set of experiments, nitrocellulose membranes were cut according to molecular weight and Western-blotted with rabbit anti-NEDD4 (Cell Signaling Technology; catalog no. 3607S) and mouse anti-β-arrestin2 (LSBio; LS-B6008).

To confirm the specificity of β-arrestin2 immunoprecipitation by rabbit anti-β-arrestin2 antibody (LSBio; LS-B15546) in drug-naïve N2A cells and rat PFC tissue, a corresponding blocking peptide (GenScript: sequence DDIVFEDFARLRLK) was used. Briefly, immunoprecipitation of β-arrestin2 was performed as described above in the presence or absence of the β-arrestin2–blocking peptide (10 μg). Immunoprecipitates and whole-cell lysate were immunoblotted for mouse anti-ubiquitin (Santa Cruz Biotechnology; sc8017) and mouse anti-β-arrestin2 (LSBio; LS-B6008).

Statistical analysis

GraphPad Prism 5 (La Jolla, CA) was used for statistical analysis. Data are presented as mean ± S.E. A two-tailed unpaired *t* test was used for MDM2 protein levels after siRNA knockdown. A one-way ANOVA followed by Bonferroni post hoc analysis was used for determining β-arrestin protein level and ubiquitination. A two-way ANOVA followed by Bonferroni post hoc analysis for multiple comparisons was used for all other experiments. A value of $p \leq 0.05$ was considered statistically significant.

Author contributions—D. J. L., B. A. M., and R. C. conceptualization; D. J. L., H. S., M. M. M., and M. H. data curation; D. J. L. software; D. J. L., H. S., and M. H. formal analysis; D. J. L., B. A. M., and R. C. funding acquisition; D. J. L. and R. C. investigation; D. J. L. and G. M. methodology; D. J. L., M. M. M., and R. C. writing-original draft; D. J. L., B. A. M., and R. C. writing-review and editing; G. M. and R. C. resources; R. C. supervision; R. C. project administration.

Acknowledgments—We thank Dr. Allyn Howlett for helpful comments during the preparation of this manuscript. Additionally, we thank the Wake Forest Center for Molecular Signaling and Wake Forest Microscopic Imaging Core Facility.

References

1. Eng, M. Y., Schuckit, M. A., and Smith, T. L. (2005) The level of response to alcohol in daughters of alcoholics and controls. *Drug Alcohol Depend.* **79,** 83–93 CrossRef Medline
2. Newlin, D. B., and Renton, R. M. (2010) High risk groups often have higher levels of alcohol response than low risk: the other side of the coin. *Alcohol Clin. Exp. Res.* **34,** 199–202; author reply, 203–205 CrossRef Medline
3. King, A. C., McNamara, P. J., Hasin, D. S., and Cao, D. (2014) Alcohol challenge responses predict future alcohol use disorder symptoms: a 6-year prospective study. *Biol. Psychiatry* **75,** 798–806 CrossRef Medline
4. King, A. C., Hasin, D., O'Connor, S. J., McNamara, P. J., and Cao, D. (2016) A prospective 5-year re-examination of alcohol response in heavy drinkers progressing in alcohol use disorder. *Biol. Psychiatry* **79,** 489–498 CrossRef Medline
5. Blomqvist, O., Söderpalm, B., and Engel, J. A. (1994) 5-HT1A receptor agonists reduce ethanol-induced locomotor activity in mice. *Alcohol* **11,** 157–161 CrossRef Medline
6. Blednov, Y. A., and Harris, R. A. (2008) Metabotropic glutamate receptor 5 (mGluR5) regulation of ethanol sedation, dependence and consumption: relationship to acamprosate actions. *Int. J. Neuropsychopharmacol.* **11,** 775–793 CrossRef Medline
7. Nguyen, P. T., Schmid, C. L., Raehal, K. M., Selley, D. E., Bohn, L. M., and Sim-Selley, L. J. (2012) β-Arrestin2 regulates cannabinoid CB1 receptor signaling and adaptation in a central nervous system region-dependent manner. *Biol. Psychiatry* **71,** 714–724 CrossRef Medline
8. Naassila, M., Pierrefiche, O., Ledent, C., and Daoust, M. (2004) Decreased alcohol self-administration and increased alcohol sensitivity and withdrawal in CB1 receptor knockout mice. *Neuropharmacology* **46,** 243–253 CrossRef Medline
9. Serrano, A., and Parsons, L. H. (2011) Endocannabinoid influence in drug reinforcement, dependence and addiction-related behaviors. *Pharmacol. Ther.* **132,** 215–241 CrossRef Medline
10. Björk, K., Rimondini, R., Hansson, A. C., Terasmaa, A., Hyytiä, P., Heilig, M., and Sommer, W. H. (2008) Modulation of voluntary ethanol consumption by β-arrestin 2. *FASEB J.* **22,** 2552–2560 CrossRef Medline
11. Shenoy, S. K., Barak, L. S., Xiao, K., Ahn, S., Berthouze, M., Shukla, A. K., Luttrell, L. M., and Lefkowitz, R. J. (2007) Ubiquitination of β-arrestin links seven-transmembrane receptor endocytosis and ERK activation. *J. Biol. Chem.* **282,** 29549–29562 CrossRef Medline
12. Kumar, P., Lau, C. S., Mathur, M., Wang, P., and DeFea, K. A. (2007) Differential effects of β-arrestins on the internalization, desensitization and ERK1/2 activation downstream of protease activated receptor-2. *Am. J. Physiol. Cell Physiol.* **293,** C346–C357 CrossRef Medline

13. Jean-Charles, P. Y., Freedman, N. J., and Shenoy, S. K. (2016) Cellular roles of β-arrestins as substrates and adaptors of ubiquitination and deubiquitination. *Prog. Mol. Biol. Transl. Sci.* **141,** 339–369 CrossRef Medline
14. Hershko, A., and Ciechanover, A. (1998) The ubiquitin system. *Annu. Rev. Biochem.* **67,** 425–479 CrossRef Medline
15. Clague, M. J., and Urbé, S. (2010) Ubiquitin: same molecule, different degradation pathways. *Cell* **143,** 682–685 CrossRef Medline
16. Shenoy, S. K., McDonald, P. H., Kohout, T. A., and Lefkowitz, R. J. (2001) Regulation of receptor fate by ubiquitination of activated β2-adrenergic receptor and β-arrestin. *Science* **294,** 1307–1313 CrossRef Medline
17. Shenoy, S. K., Modi, A. S., Shukla, A. K., Xiao, K., Berthouze, M., Ahn, S., Wilkinson, K. D., Miller, W. E., and Lefkowitz, R. J. (2009) β-Arrestin-dependent signaling and trafficking of 7-transmembrane receptors is reciprocally regulated by the deubiquitinase USP33 and the E3 ligase MDM2. *Proc. Natl. Acad. Sci. U.S.A.* **106,** 6650–6655 CrossRef Medline
18. Lin, C. H., MacGurn, J. A., Chu, T., Stefan, C. J., and Emr, S. D. (2008) Arrestin-related ubiquitin-ligase adaptors regulate endocytosis and protein turnover at the cell surface. *Cell* **135,** 714–725 CrossRef Medline
19. Akutsu, M., Dikic, I., and Bremm, A. (2016) Ubiquitin chain diversity at a glance. *J. Cell Sci.* **129,** 875–880 CrossRef Medline
20. Jura, N., Scotto-Lavino, E., Sobczyk, A., and Bar-Sagi, D. (2006) Differential modification of Ras proteins by ubiquitination. *Mol. Cell* **21,** 679–687 CrossRef Medline
21. Golan, M., Schreiber, G., and Avissar, S. (2010) Antidepressants increase β-arrestin 2 ubiquitinylation and degradation by the proteasomal pathway in C6 rat glioma cells. *J. Pharmacol. Exp. Ther.* **332,** 970–976 CrossRef Medline
22. Fornai, F., Lenzi, P., Capobianco, L., Iacovelli, L., Scarselli, P., Lazzeri, G., and De Blasi, A. (2008) Involvement of dopamine receptors and beta-arrestin in methamphetamine-induced inclusions formation in PC12 cells. *J. Neurochem.* **105,** 1939–1947 CrossRef Medline
23. Wolfe, S. A., Workman, E. R., Heaney, C. F., Niere, F., Namjoshi, S., Cacheaux, L. P., Farris, S. P., Drew, M. R., Zemelman, B. V., Harris, R. A., and Raab-Graham, K. F. (2016) FMRP regulates an ethanol-dependent shift in GABABR function and expression with rapid antidepressant properties. *Nat. Commun.* **7,** 12867 CrossRef Medline
24. Méndez, M., Leriche, M., and Calva, J. C. (2001) Acute ethanol administration differentially modulates μ opioid receptors in the rat meso-accumbens and mesocortical pathways. *Brain Res. Mol. Brain Res.* **94,** 148–156 CrossRef Medline
25. Rojas, P. S., and Fiedler, J. L. (2016) What do we really know about 5-HT1A receptor signaling in neuronal cells? *Front. Cell. Neurosci.* **10,** 272 CrossRef Medline
26. Kelaï, S., Renoir, T., Chouchana, L., Saurini, F., Hanoun, N., Hamon, M., and Lanfumey, L. (2008) Chronic voluntary ethanol intake hypersensitizes 5-HT(1A) autoreceptors in C57BL/6J mice. *J. Neurochem.* **107,** 1660–1670 CrossRef Medline
27. Zhou, F. C., McKinzie, D. L., Patel, T. D., Lumeng, L., and Li, T. K. (1998) Additive reduction of alcohol drinking by 5-HT1A antagonist WAY 100635 and serotonin uptake blocker fluoxetine in alcohol-preferring P rats. *Alcohol Clin. Exp. Res.* **22,** 266–269 CrossRef Medline
28. Burnett, E. J., Grant, K. A., Davenport, A. T., Hemby, S. E., and Friedman, D. P. (2014) The effects of chronic ethanol self-administration on hippocampal 5-HT1A receptors in monkeys. *Drug Alcohol Depend.* **136,** 135–142 CrossRef Medline
29. Shenoy, S. K., and Lefkowitz, R. J. (2005) Receptor-specific ubiquitination of β-arrestin directs assembly and targeting of seven-transmembrane receptor signalosomes. *J. Biol. Chem.* **280,** 15315–15324 CrossRef Medline
30. Shenoy, S. K., and Lefkowitz, R. J. (2003) Trafficking patterns of β-arrestin and G protein-coupled receptors determined by the kinetics of β-arrestin deubiquitination. *J. Biol. Chem.* **278,** 14498–14506 CrossRef Medline
31. Seyfried, N. T., Xu, P., Duong, D. M., Cheng, D., Hanfelt, J., and Peng, J. (2008) Systematic approach for validating the ubiquitinated proteome. *Anal. Chem.* **80,** 4161–4169 CrossRef Medline
32. Della Rocca, G. J., Mukhin, Y. V., Garnovskaya, M. N., Daaka, Y., Clark, G. J., Luttrell, L. M., Lefkowitz, R. J., and Raymond, J. R. (1999) Serotonin 5-HT1A receptor-mediated Erk activation requires calcium/calmodulin-dependent receptor endocytosis. *J. Biol. Chem.* **274,** 4749–4753 CrossRef Medline
33. Smith, J. S., and Rajagopal, S. (2016) The β-arrestins: multifunctional regulators of G protein-coupled receptors. *J. Biol. Chem.* **291,** 8969–8977 CrossRef Medline
34. Luessen, D. J., Hinshaw, T. P., Sun, H., Howlett, A. C., Marrs, G., McCool, B. A., and Chen, R. (2016) RGS2 modulates the activity and internalization of dopamine D2 receptors in neuroblastoma N2A cells. *Neuropharmacology* **110,** 297–307 CrossRef Medline
35. Bouaziz, E., Emerit, M. B., Vodjdani, G., Gautheron, V., Hamon, M., Darmon, M., and Masson, J. (2014) Neuronal phenotype dependency of agonist-induced internalization of the 5-HT(1A) serotonin receptor. *J. Neurosci.* **34,** 282–294 CrossRef Medline
36. Lindblad, J., Wählby, C., Bengtsson, E., and Zaltsman, A. (2004) Image analysis for automatic segmentation of cytoplasms and classification of Rac1 activation. *Cytometry A* **57,** 22–33 CrossRef Medline
37. Dimopoulos, S., Mayer, C. E., Rudolf, F., and Stelling, J. (2014) Accurate cell segmentation in microscopy images using membrane patterns. *Bioinformatics* **30,** 2644–2651 CrossRef Medline
38. Ferrer-Alcón, M., La Harpe, R., and García-Sevilla, J. A. (2004) Decreased immunodensities of micro-opioid receptors, receptor kinases GRK 2/6 and β-arrestin-2 in postmortem brains of opiate addicts. *Brain Res. Mol. Brain Res.* **121,** 114–122 CrossRef Medline
39. Fan, X. L., Zhang, J. S., Zhang, X. Q., Yue, W., and Ma, L. (2003) Differential regulation of β-arrestin 1 and β-arrestin 2 gene expression in rat brain by morphine. *Neuroscience* **117,** 383–389 CrossRef Medline
40. Amm, I., Sommer, T., and Wolf, D. H. (2014) Protein quality control and elimination of protein waste: the role of the ubiquitin-proteasome system. *Biochim. Biophys. Acta* **1843,** 182–196 CrossRef Medline
41. Ranaweera, R. S., and Yang, X. (2013) Auto-ubiquitination of MDM2 enhances its substrate ubiquitin ligase activity. *J. Biol. Chem.* **288,** 18939–18946 CrossRef Medline
42. Chakrabarti, S., Oppermann, M., and Gintzler, A. R. (2001) Chronic morphine induces the concomitant phosphorylation and altered association of multiple signaling proteins: a novel mechanism for modulating cell signaling. *Proc. Natl. Acad. Sci. U.S.A.* **98,** 4209–4214 CrossRef Medline
43. Hillmer, A. T., Wooten, D. W., Tudorascu, D. L., Barnhart, T. E., Ahlers, E. O., Resch, L. M., Larson, J. A., Converse, A. K., Moore, C. F., Schneider, M. L., and Christian, B. T. (2014) The effects of chronic alcohol self-administration on serotonin-1A receptor binding in nonhuman primates. *Drug Alcohol Depend.* **144,** 119–126 CrossRef Medline
44. Nevo, I., Langlois, X., Laporte, A. M., Kleven, M., Koek, W., Lima, L., Maudhuit, C., Martres, M. P., and Hamon, M. (1995) Chronic alcoholization alters the expression of 5-HT1A and 5-HT1B receptor subtypes in rat brain. *Eur. J. Pharmacol.* **281,** 229–239 CrossRef Medline
45. Hicke, L. (2001) Protein regulation by monoubiquitin. *Nat. Rev. Mol. Cell Biol.* **2,** 195–201 CrossRef Medline
46. Lauwers, E., Erpapazoglou, Z., Haguenauer-Tsapis, R., and André, B. (2010) The ubiquitin code of yeast permease trafficking. *Trends Cell Biol.* **20,** 196–204 CrossRef Medline
47. Ziv, I., Matiuhin, Y., Kirkpatrick, D. S., Erpapazoglou, Z., Leon, S., Pantazopoulou, M., Kim, W., Gygi, S. P., Haguenauer-Tsapis, R., Reis, N., Glickman, M. H., and Kleifeld, O. (2011) A perturbed ubiquitin landscape distinguishes between ubiquitin in trafficking and in proteolysis. *Mol. Cell. Proteomics* **10,** M111.009753 CrossRef Medline
48. Hicke, L., and Dunn, R. (2003) Regulation of membrane protein transport by ubiquitin and ubiquitin-binding proteins. *Annu. Rev. Cell Dev. Biol.* **19,** 141–172 CrossRef Medline
49. Li, X., Léetourneau, D., Holleran, B., Leduc, R., Lavigne, P., and Lavoie, C. (2017) Gαs protein binds ubiquitin to regulate epidermal growth factor receptor endosomal sorting. *Proc. Natl. Acad. Sci. U.S.A.* **114,** 13477–13482 CrossRef Medline
50. Violin, J. D., Ren, X. R., and Lefkowitz, R. J. (2006) G-protein-coupled receptor kinase specificity for β-arrestin recruitment to the β2-adrenergic receptor revealed by fluorescence resonance energy transfer. *J. Biol. Chem.* **281,** 20577–20588 CrossRef Medline

51. Daigle, T. L., Kwok, M. L., and Mackie, K. (2008) Regulation of CB1 cannabinoid receptor internalization by a promiscuous phosphorylation-dependent mechanism. *J. Neurochem.* **106,** 70–82 CrossRef Medline
52. Reiter, E., and Lefkowitz, R. J. (2006) GRKs and β-arrestins: roles in receptor silencing, trafficking and signaling. *Trends Endocrinol. Metab.* **17,** 159–165 CrossRef Medline
53. Läck, A. K., Diaz, M. R., Chappell, A., DuBois, D. W., and McCool, B. A. (2007) Chronic ethanol and withdrawal differentially modulate pre- and postsynaptic function at glutamatergic synapses in rat basolateral amygdala. *J. Neurophysiol.* **98,** 3185–3196 CrossRef Medline
54. Morales, M., McGinnis, M. M., Robinson, S. L., Chappell, A. M., and McCool, B. A. (2018) Chronic intermittent ethanol exposure modulation of glutamatergic neurotransmission in rat lateral/basolateral amygdala is duration-, input-, and sex-dependent. *Neuroscience* **371,** 277–287 CrossRef Medline
55. Blevins, T., Mirshahi, T., Chandler, L. J., and Woodward, J. J. (1997) Effects of acute and chronic ethanol exposure on heteromeric *N*-methyl-D-aspartate receptors expressed in HEK 293 cells. *J. Neurochem.* **69,** 2345–2354 Medline
56. Chandler, L. J., Newsom, H., Sumners, C., and Crews, F. (1993) Chronic ethanol exposure potentiates NMDA excitotoxicity in cerebral cortical neurons. *J. Neurochem.* **60,** 1578–1581 CrossRef Medline
57. Xiao, X., Zi, X. D., Niu, H. R., Xiong, X. R., Zhong, J. C., Li, J., Wang, L., and Wang, Y. (2014) Effect of addition of FSH, LH and proteasome inhibitor MG132 to *in vitro* maturation medium on the developmental competence of yak (*Bos grunniens*) oocytes. *Reprod. Biol. Endocrinol.* **12,** 30 CrossRef Medline